A major purpose of the Tecr cal Information Center is to provi the broadest dissemination pos ble of information contained DOE's Research and Developme Reports to business, industry, t academic community, and feder state and local governments.

Although a small portion of tl report is not reproducible, it being made available to exped the availability of information on t research discussed herein.

LA-UR--83-3288

DE84 003798

CONF-830918--4

TITLE: A LINAC-DRIVEN XUV FREE-ELECTRON LASER

AUTHOR(S): Brian E. Newnam, CHM-6
John C. Goldstein, X-1
John S. Fraser, AT-7
Richard K. Cooper, AT-6

SUBMITTED TO: Proceedings of the Optical Society of America Topical Meeting on Free-Electron Generation of Extreme Ultraviolet Coherent Radiation, held at Brookhaven National Laboratory, Upton, Long Island, New York, Sept. 19-22, 1983

Los Alamos National Laboratory
Los Alamos, New Mexico 87545

FORM NO 836 R4
ST NO 2629 5/81

A LINAC-DRIVEN XUV FREE-ELECTRON LASER

Brian E. Newnam, John C. Goldstein,
John S. Fraser, and Richard K. Cooper
Chemistry Division
Los Alamos National Laboratory
Los Alamos, New Mexico 87545

ABSTRACT

Use of an rf linear accelerator as the electron source for a free-electron laser operating in the extreme ultraviolet wavelength range from 100 nm to at least as low as 50 nm appears feasible. Peak and average power outputs of greater than 100 kW and 50 W, respectively, are predicted.

INTRODUCTION

Broadly-tunable sources of extreme ultraviolet (XUV) radiation are in great demand for a multitude of basic physics and materials studies.[1,2] For the spectral range below 100 nm, electron synchrotrons are currently the dominant radiation source for such research. However, there are a number of "photon-hungry" experiments (involving nonlinear XUV spectroscopy, for example) which can be pursued only at substantially higher ($>10^3$ X) intensities than provided by synchrotrons including those with undulator or wiggler sections [3]

Recently, several laser-driven processes (harmonic generation and frequency mixing) have produced coherent XUV radiation with much higher brightness (watts/mr$\cdot$cm^{-1}), but with very limited tunability.[4,5] To obtain greater spectral coverage with the requisite high brightness, attention has now turned to the free-electron laser (FEL) as a potential XUV generator.[6] At such short wavelengths, an FEL requires an electron accelerator capable of high-peak current and very restricted beam emittance and energy spread. The electron storage ring may well satisfy these requirements, and design considerations are reviewed by J. Madey elsewhere in these proceedings.[7]

As an alternative to the storage-ring approach, we consider here the use of an rf linear accelerator in an XUV laser system. Inherently less complicated and less costly than with a storage ring, a linac-driven FEL appears to be feasible for wavelengths as short as 50 nm. This projection is based upon the anticipated successful use of high-peak current (~100 A) linacs in present and forthcoming FEL oscillator experiments at infrared and visible wavelengths by Los Alamos and Boeing/Mathematical Sciences

Northwest.[8,9] An important feature of the linac approach is that electrons pass through the undulator magnet only once, but their energy may be recovered in a separate decelerating structure and fed back into the primary accelerator. Another advantage is the option of unrestricted undulator length. As with storage rings, rf linacs are capable of high-peak currents up to 1000 A,[10] but with shorter bunch lengths of 10-50 ps, FWHM. The major concern with rf linacs is the attainment of sufficiently-low transverse beam emittance. Additionally, since each electron bunch must be accelerated from rest, the linac must be operated at a moderate duty factor, e.g. 5%, to maintain rf power costs at a reasonable level. In the following section we describe the properties of an undulator and the electron beam necessary to attain sufficient optical gain for the 50- to 100-nm spectral range. We then compare these necessary beam properties with those of existing rf linacs. With an upper bound on the transverse emittance, we next predict the peak- and average-power output from an optical cavity designed for this application. Finally, a scheme for electron energy recovery is outline followed by our overall conclusions.

UNDULATOR AND ELECTRON BEAM PROPERTIES

The basis for scaling parameters from the current Los Alamos 10-μm oscillator experiment[8] to conditions suitable for an XUV free-electron laser is the Colson formula[11] for the maximum small-signal gain of an FEL comprised of a plane-polarized, constant-period undulator driven by a perfectly monoenergetic electron beam,

$$G_{max} = 0.135\, e^4 B_w^2 \lambda_w n_e (L_w/\gamma mc^2)^3 [J_o(\xi) - J_1(\xi)]^2 \quad , \qquad (1)$$

where $\xi \equiv a_w^2/(4 + 2a_w^2)$ and $a_w = eB_w\lambda_w/2\pi mc^2$, B_w is the peak magnetic field on axis, λ_w is the undulator period, and ρ_e is the electron charge density. In particular, the formula predicts that the gain should remain constant if both the undulator length L_w and the electrons' relativistic energy factor γ both increase by the same factor. Increasing γ by a factor of 10 (from 40 to 400) reduces the resonant optical wavelength by a factor of 100 for the same magnet parameters B_w and λ_w. In fact, one can obtain very high magnetic fields for small ratios of the magnet gap to period according to Halbach's undulator design using $SmCo_5$ permanent magnets.[12] The design parameters for the XUV undulator are given in Table I.

It should be noted that these undulator parameters represent a sufficient design (when accompanied by the electron beam and optical cavity parameters specified below), that is, one with sufficient gain to achieve oscillation. No attempt at further optimization has been done. This single undulator so specified will work in the 50-100-nm region, but it might be advantageous, if tunability over this entire region is not required, to further optimize the design for a particular operating wavelength.

The Colson formula[11] is based on perturbation theory and is quantitatively valid only when the value of the maximum gain is itself a small number, $\lesssim 0.2$. When parameters are such that the formula gain is not small, then account must be taken of the change in amplitude of the radiation field during a single pass through the interaction region.[13,14]

TABLE I

Parameters of a Plane-Polarized, Uniform-Period Magnetic Undulator

L_W = 1200 cm

B_W = 7.5 T

λ = 1.6 cm

a_W = 1.12

gap = 3.7 mm

The analytical gain formula Eq. (1) provides valuable insight into the relative dependence on undulator and electron beam parameters, but it becomes very inaccurate for large values of gain. For example, for a monoenergetic beam with peak current of 100 A and with other parameters appropriate for an 82-nm FEL, Eq. (1) underestimates the actual gain by a factor of 60! However, when the electron beam has a non-zero energy spread, the difference between analytical and numerical calculations of gain is less dramatic. For a 1% energy spread, the numerically-calculated gain drops substantially from over 3000 to 3.4 as shown in Fig. 1, whereas that predicted by Eq. (1) (modified by a broadening factor[15,16]) falls to a value of 2.2 which is only 35% too small. For the high, weak signal gains (>100%) necessary to overcome mirror losses in the XUV, and with significantly broad electron energy distributions, we henceforth rely only on numerical calculations of the gain.

Having seen in Fig. 1 the drastic reduction of small-signal gain by inhomogeneous broadening, one must make substantial efforts to minimize the energy spread of the electron beam. One source of such spread is due to the finite pulse duration of the electron beam. Some electrons are driven by accelerating fields slightly less than the peak value because they arrive at the accelerating gaps slightly before or after the moment of maximum field. This leads to a spread of energies in the pulse. However, by energy-scraping with a slit in a dispersive section of the beam transport, this spread can be reduced to a small value at the expense of some beam current. Hence, it is ignored in the considerations below.

The important remaining source of energy spread in an rf linac appears to be due to the finite emittance of the electron beam. The beam emittance leads to an effective energy spread in the indulator which is the sum of two separate contributions: one depending on the angular divergence of the beam, and the other depending on the beam size.[17] The divergence implies a spread of electron z-velocities, and the finite size of the beam implies that some electron trajectories are displaced away from the undulator axis into regions of higher magnetic field strength which results in correspondingly slower z-velocities as well. The sum of the effective energy spreads due to these two effects is written as

$$\left(\frac{\delta\gamma}{\gamma}\right)_{tot} = \left(\frac{\delta\gamma}{\gamma}\right)_{\varepsilon} + \left(\frac{\delta\gamma}{\gamma}\right)_{size} , \tag{2}$$

and is minimized for a particular value of the beam radius given by

$$A_b^2\Big|_{min} = \frac{\gamma\varepsilon\lambda_w}{\sqrt{2}\pi^2 a_w} . \tag{3}$$

The corresponding total effective energy spread is ther

$$\left(\frac{\delta\gamma}{\gamma}\right)_{Tot/min} = \frac{\varepsilon a_w}{\sqrt{2}\gamma\lambda_s} \quad . \tag{4}$$

From the calculations of gain vs inhomogeneous broadening, it appears that an energy spread of 1% may be tolerated and still allow laser oscillation. Assuming this value as the minimum effective energy spread in Eq.(4), there is a corresponding value of the beam emittance ε as well as a beam radius $r_b^2\big|_{min}$ for particular values of γ, λ_s, and magnet parameters.

~~Is the value of $r_b^2\big|_{min}$ just prescribed attainable?~~ If the focusing by the undulator magnet array itself is neglected for the moment, we can evaluate focusing of the beam in the undulator by an external, magnetic quadrupole system. To accommodate a plane wave calculation with our 1-D numerical code, it is necessary to determine the average value of the beam radius within the undulator. This average value is easily determined from the well-known beam propagation expression from which a minimum average radius $\langle r^2\rangle$ is determined to be

$$\langle r^2\rangle_{min} = \varepsilon L_w/\sqrt{3}\pi \quad . \tag{5}$$

Using the emittance values deduced above and the undulator parameters listed in Table I, we found that external focusing of the beam into the undulator did not obtain a small enough value of $\langle r^2\rangle_{min}$ ($\leq r_b^2\big|_{min}$) to achieve the desired condition of minimal effective broadening. However, by focusing the electron beam not once but several times within the undulator by use of a series of external quadrupoles around the undulator,

a smaller value of $\langle r^2 \rangle_{min}$ can be achieved. (The magnetic fields of external quadrupoles superpose linearly over the undulator field for an all-$SmCo_5$ permanent magnet structure. This would not be the case for hybrid undulators containing some iron.)[12] For three focal points in the undulator, $\langle r^2 \rangle_{min} = \varepsilon L_w / 3\sqrt{3}\pi$. Using this latter value, we evaluated the two effective energy spread terms in Eq. (2) separately to arrive at a total effective energy spread. The final system parameters are shown in Table II where it is clear that the broadening only slightly exceeds the target value of 1%.

For a given emittance, minimization of the average beam size is very important for two reasons: (1) the effective broadening is usually reduced, and (2) higher electron density increases the gain as seen in Eq. (1). External focusing to keep the beam diameter small appears to be feasible, as shown in Fig. 2 which is the result of a calculation of the size of a beam (for an 82-nm FEL) propagating through a series of 30 quadrupoles which focus alternately in the two transverse planes. The necessary magnetic field strengths of the quads are quite low, ≤100 G.

The single-pass gain was calculated numerically for the parameters listed in Table II and as a function of input intensity. Figure 3 shows the gain curves for three XUV wavelengths, and it is evident that gain saturation occurs at higher intensities for shorter wavelengths. A qualitative explanation is that gain saturation occurs when electrons contained within the energy/phase area (called a "bucket") change energy by ~1/2 the bucket height. This happens when the undulator length is approximately equal to half of a synchrotron period L_{sy}. L_{sy}, in turn, is inversely proportional to the product of the optical electric field E and the optical wavelength λ_s via the relation $(E\lambda_s)^{-1/2}$. This reveals that the condition $L_{sy} = 2\ L_w$ is reached at lower values of the electric field for longer wavelengths.

We note, for later reference, that the onset of sideband-frequency generation[18] occurs for $L_{sy} \approx L_w$. At the three wavelengths 50, 82, and 101 nm, this condition occurs at intensities of about 1.13, 0.43, and 0.28 GW/cm^2, respectively. We further observe that, despite the large peak current of 100 A, existing theories[11,14] for the onset of Coulomb effects predict that our parameters are about a factor of 20 below those for which such effects appear.

TABLE II

ELECTRON BEAM PARAMETERS

	50 nm	82 nm	101 nm
γ	510	400	361
I, A	100	100	100
ε/π, cm. rad	1.03×10^{-5}	1.30×10^{-5}	1.45×10^{-5}
d, cm	0.0973	0.110	0.116
$\delta\gamma/\gamma$, %	1.06	1.18	1.25

COMPARISON WITH EXISTING LINACS

Having determined the electron beam current and emittance necessary for FEL oscillation in the XUV, it is enlightening to compare these properties with those of recently-constructed linacs. The often-cited Lawson-Penner relationship[19] empirically describes the average performance of linear accelerators in terms of transverse emittance and current averaged over an acceleration cycle

$$(\beta\gamma\varepsilon/\pi)^2 = 0.9 \times 10^{-4}\ \bar{I}\ (\text{cm}\cdot\text{rad}) \quad . \tag{6}$$

Actually, emittance is physically related to the peak current in each micropulse accelerated. Presumably, Eq. (6) is given in terms of the average current because the microbunch pulsewidth of linacs is rarely directly measured.

Next best to having a relationship in terms of peak current is one involving Q the charge per bunch as

$$(\beta\gamma\varepsilon/\pi)^2 = 0.9 \times 10^{-4} fQ\ (\text{cm}\cdot\text{rad}) \quad , \tag{7}$$

where f is the rf frequency of the accelerator. In these terms, Fig. 4 presents a comparison of the normalized emittance squared versus Q for a number of existing L- and S-band linacs. Curves for the modified Lawson-Penner relationship, Eq. (7), are shown for reference. It is apparent that present linac emittance is about a factor of three better than described by the empirical average of Eq. (7). Also apparent is the large amount of emittance growth: starting from the thermal limit of dispenser-cathode emission, to the triode-gun output, and to that of the linac. Obviously, there is room for a great amount of improvement! Nevertheless, the optical gain curves shown in Fig. 3 were computed with emittance values (Table II) represented by the starred circle in Fig. 4. This emittance is equivalent to recent high-current performance of L-band accelerators at Argonne[10] and Los Alamos National Laboratories (data not plotted).[25]

One scheme to realize low emittance is a laser-irradiated photocathode by which, as indicated in Fig. 4, a large current density may be attained within a short laser pulse. In pioneering work at SLAC, Sinclair and Miller have has obtained 60 A from a GaAs cathode.[24,10] Laboratory studies with cesiated surfaces also show promise for use as gun cathodes.[26] By using ~30-ps laser irradiation on such surfaces and immediately accelerating the charge to high velocity through a 200 kV - 1 MV potential within a Pierce-geometry cavity, it is possible both to attain high peak current and to eliminate the pulse-forming bunching sections which are often cited as the source of substantial emittance growth. A laser-irradiated cathode injector-development program has been initiated at Los

XUV FEL LASER POWER OUTPUT

An oscillator configuration designed for wavelengths longer than about 50 nm is shown in Fig. 5. For the normal-incidence end mirrors, multilayer stacks of atomic materials such as tungsten and carbon are used. According to T. Barbee[24-27] of Stanford University, multilayer mirror reflectance of 80% should be attainable with present state-of-the-art coating technology applicable to the 50-100-nm spectral range.

To avoid thermal distortion or catastrophic damage to the end mirrors, intracavity grazing-incidence reflectors with slight curvature diverge the optical radiation to an adequately-low power density. The advantages of grazing-incidence mirrors have been explored previously for 248 nm and 10.6 μm by Mumola and Jordan.[28] Chemically-vapor deposited SiC was chosen for these mirrors because of its high thermal figure of merit, K/α, of 5 x 10^5 W/cm and its unsurpassed reflectance for ultraviolet wavelengths between 50 and 110 nm.[29] The SiC intracavity mirrors are radially curved in only one plane to assure only S-plane reflectance which, for 88° incidence, is 97%.[30] P-plane polarization with its lower reflectance and, thereby, higher absorption is thus avoided. Output coupling through a central hole in the exit mirror was chosen over edge coupling for ease of mirror mounting.

The peak power output as a function of cavity mirror reflectance, shown in Fig. 6, has been maximized by optimizing the output coupling fraction. For a reflectance of 80%, peak powers of 180 and 350 kW at 50 and 101 nm, respectively, have been predicted. If the multilayer reflector technology improves sufficiently to reach 90% reflectances, 500 kW peak power may be attained. On the other hand, smaller but substantial

power is still calculated for reflectances lower than 70%. Thermal distortion of the SiC grazing-incidence mirror nearest the output coupler limits the average power output of this system. For thermal distortion less than 1/20 wave at each respective wavelength, an average output power of 200 W is computed for repetitive pulses every 25-50 ns.

ELECTRON ENERGY RECOVERY

To accelerate a 30-ps, 100-A peak current microbunch to 200 MeV continuously every 25 ns requires 24 MW of effective rf beam power. Since the energy extraction efficiency at the saturation intensity of 100 MW/cm^2 is only 10^{-4}, the electrons experience negligible net deceleration within the undulator. Therefore, it is very advantageous economy-wise to recover this energy.# In his review of FEL fundamentals, Brau[31] described several possible methods of energy recovery. In the racetrack scheme, electrons exiting the undulator are reinserted into the accelerator 180° out of phase. The rf power radiated by the decelerating electrons then serves to accelerate new, succeeding electron bunches. Theoretically, 195 MeV of the original electron energy of a 200 MeV beam can be recovered.[32] On the average, this translates to recovery of 21 MW out of 24 MW beam power. However, to the 3 MW lost, must be added power dissipated in the copper accelerating structures. Copper losses depend upon the accelerating gradient and amount to 22 MW (11 MW) for a 25-m (8?-m) long accelerator.[32] The net average power to obtain 200 W of XUV power is 25 MW or 14 MW depending on which of the two gradients is chosen. By operating with a duty factor of 5%, it is still possible to obtain 50 W of average XUV radiation (peak power output remains the same) whil the total rf power expense is about 1 MW. This rf power requirement is equal to that of the National Light Source VUV storage ring at Brookhaven National Laboratory.[33]

CONCLUSIONS

RF linacs appear as feasible electron sources for free-electron lasers operating in the XUV wavelength range of 50 to 100 nm if a moderate reduction in beam emittance (a factor of 2) can be attained over current machine performance. High peak current of the order of 100 A and more with an energy spread of no more than 0.5% will be required. With peak power and average power output greater than 100 kW and 50 W, respectively, such a laser would surpass the capabilities of any existing, continuously-tunable XUV source by three to four orders of magnitude. Such a photon source should be attractive for a great variety of scientific applications.

ACKNOWLEDGMENTS

The authors are pleased to acknowledge the helpful suggestions of other participants in the current Los Alamos FEL experiments which include C. A. Brau, R. L. Sheffield, W. E. Stein, R. W. Warren, and J. M. Watson. Particular thanks go to J. M. Watson for supplying the energy-recovery projections.

REFERENCES

1. A. Bienenstock and H. Winick, Physics Today 36, 48 (1983).
2. H. Winick and S. Doniach, Synchrotron Radiation Research (Plenum Press, New York) 1980.
3. M. Howells, Applications Working Group Summary, Opt. Soc. Am. Topical Conf. on Free-Electron Generation of Extreme Ultraviolet Coherent Radiation, Brookhaven Nat'l. Lab., Upton, New York, Sept. 19-22, 1983.
4. T. Srinivasan, H. Egger, H. Pummer, and C. K. Rhodes, IEEE J. Quantum Electron. QE-19, 1270 (1983).
5. E. E. Marinero, C. T. Rettner, R. N. Zare, and A. H. Kung, Chem. Phys. Let. 95, 486 (1983).
6. Opt. Soc. Am. Topical Conf. on Free-Electron Generation of Extreme Ultraviolet Coherent Radiation, op. cit.
7. J. M. J. Madey, ibid.
8. R. W. Warren, J. S. Fraser, W. E. Stein, J. G. Winston, T. A. Swann, A. Lumpkin, R. L. Sheffield, J. E. Sollid, B. E. Newnam, C. A. Brau, and J. M. Watson, in Free-Electron Generators of Coherent Radiation, C. A. Brau and M. O. Scully, eds., SPIE Vol. 453, to be published, 1983.
9. W. M. Grossman, J. M. Slater, D. C. Quimby, T. L. Churchill, J. Adamski, R. C. Kennedy, and D. R. Shoffstall, SPIE Vol. 453, op. cit., (1983).
10. C. Mavrogenes, W. Gallagher, T. Kohe, and D. Ficht, IEEE Trans. Nucl. Sci. NS-30, 2989 (1983).
11. W. B. Colson, in Novel Sources of Coherent Radiation, Phys. of Quantum Electron., Vol. 5, S. F. Jacobs, M. Sargent III, and M. O. Scully, eds., (Addison-Wesley, Reading, MA), 1978, p. 157, and J. Quantum Electron. QE-17, 1417 (1981).
12. K. Halbach, J. Physique, Colloque C1, Suppl. 2, 44, C1-211 (1983).
13. C. C. Shih and A. Yariv, J. Quantum Electron. QE-17, 1387 (1981).
14. C. C. Shih in Free-Electron Generators of Coherent Radiation, SPIE Vol. 453, op. cit.

15. W. B. Colson and S. K. Ride, in Free-Electron Generators of Coherent Radiation, Phys. of Quantum Electron., Vol. 7, S. F. Jacobs, H. S. Pilloff, M. Sargent III, M. O. Scully, and R. Spitzer, eds., (Addison-Wesley, Reading, MA), 1980, p. 377.

16. C. A. Brau, IEEE J. Quantum Electron. QE-16, 335 (1980).

17. C. A. Brau and R. K. Cooper, in Free-Electron Generators of Coherent Radiation, Vol. 7, op. cit., p. 647.

18. J. C. Goldstein and W. B. Colson, in Proc. of Lasers '82 Conf., to be published, 1983.

19. V. K. Neil, "Emittance and Transport of Electron Beams in a Free-Electron Laser," SRI Tech. Rept. JSR 79-10 (December 1979), p. 6.

20. M. B. James, J. E. Clendenin, S. D. Ecklund, R. H. Miller, J. C. Sheppard, C. K. Sinclair, and J. Sodja, IEEE Trans. Nucl. Sci. NS-30, 2992 (1983).

21. J. S. Fraser and S. O. Schriber, eds, Compendium of Linear Accelerators-1976, Chalk River Rept. AECL-5156 - check

22. R. W. Warren, B. E. Newnam, J. G. Winston, W. E. Stein, L. M. Young, and C. A. Brau, IEEE J. Quantum Electron. QE-19, 391 (1983).

23. Litton Industries triode gun specification literature.

24. C. K. Sinclair and R. H. Miller, IEEE Trans. Nucl. Sci. NS-28, 2649 (1981).

25. Recent L-band accelerator performance at Los Alamos National Laboratory: Q = 1.5 nC/bunch, $\beta\gamma\varepsilon/\pi$ = 8 x 10^{-5} cm·rad, ~2% full energy spread, γ = 41.

26. P. E. Oettinger, Laser Focus 19, 10 (1983).

27. P. B. Mumola and D. C. Jordan, in Los Alamos Conf. on Optis '81, D. L. Liebenberg, ed., SPIE Vol 288, 54 (1981).

28. T. Barbee, Stanford University, private communication.

29. R. E. Engdahl, in Reflecting Optics for Synchrotron Radiation, SPIE Vol. 315, 103 (1981).

30. J. C. Rife and J. F. Osantowski, ibid, p. 103.

31. C. A. Brau, Laser Focus 17, 48 (1981).

32. J. M. Watson, Los Alamos National Laboratory, private communication.

33. A. Von Steenbergen, Brookhaven National Laboratory, private communication.

FIGURES

Fig. 1. Small-signal gain versus electron beam energy spread (inhomogneous broadening) for an 80-nm FEL. Undulator parameters ae given in Table I.

Fig. 2. Quadrupole channel for a 12-m undulator. Fixteen quadrupole doublets focus the electron beam alternately in the x- and y-planes. A length-averaged beam radius of 0.41 ± 0.077 mm results for an energy of 200 MeV and emittance ε/π of 1.3×10^{-5} cm•rad.

~~Figures (continued)~~

Fig. 3. Intensity gain versus input intensity for three XUV wavelengths.

Fig. 4. Normalized emittance squared versus electron charge per bunch for various high-current linacs. L-Band: ANL[10] and LANL[22]; S-Band: SLAC[20,21] and Boeing.[9] Respective Lawson-Penner curves ar shown for comparison.

Fig. 5. An XUV free-electron laser oscillator.

Fig. 6. Free-electron laser peak output power versus cavity mirror reflectance for three XUV wavelengths.

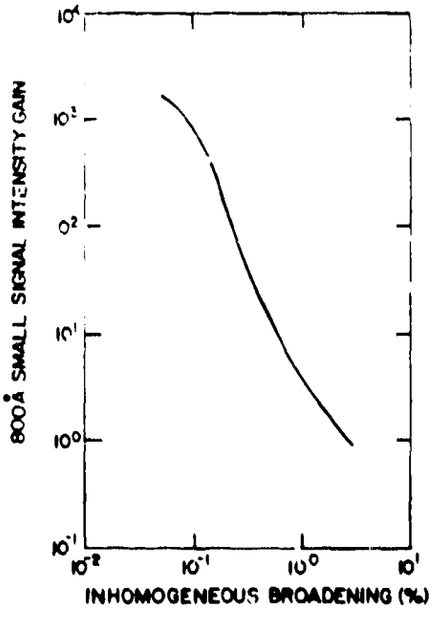
800Å SMALL SIGNAL INTENSITY GAIN
INHOMOGENEOUS BROADENING (%)

Fig. 1

Fig. 2

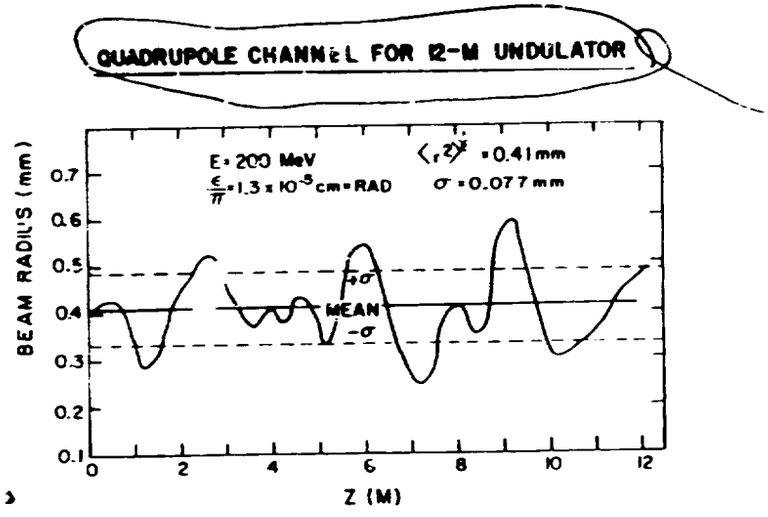
QUADRUPOLE CHANNEL FOR 12-M UNDULATOR
E = 200 MeV
$\frac{\epsilon}{\pi} = 1.3 \times 10^{-5}$ cm-RAD
$\langle r^2 \rangle^{\frac{1}{2}} = 0.41$ mm
$\sigma = 0.077$ mm
+σ
MEAN
-σ
BEAM RADIUS (mm)
0.7
0.6
0.5
0.4
0.3
0.2
0.1
0
2
4
6
8
10
12
Z (M)

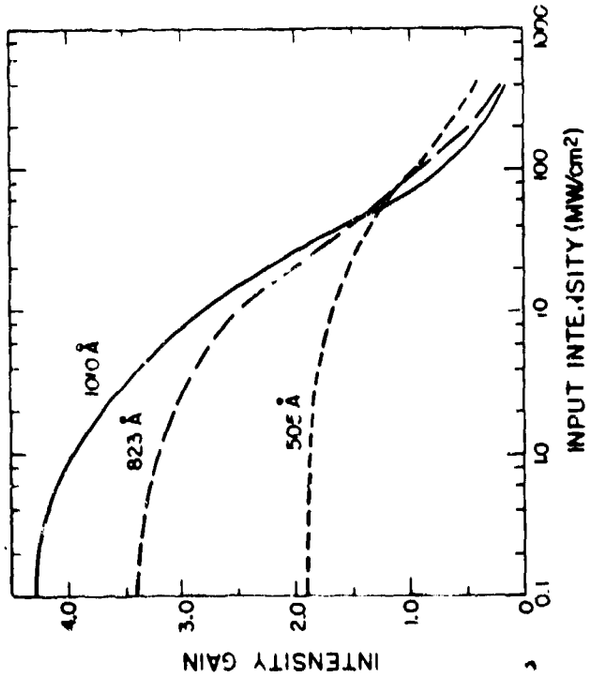
INTENSITY GAIN
4.0
3.0
2.0
1.0
0
0.1
1.0
10
100
1000
INPUT INTENSITY (MW/cm²)
1000 Å
823 Å
500 Å

Fig. 3.

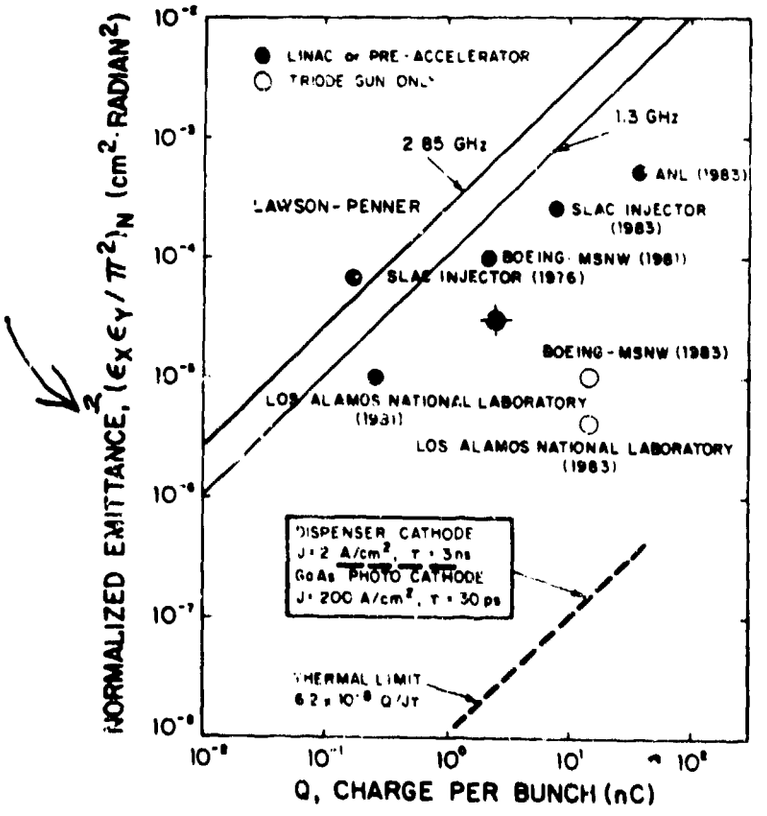
LINAC or PRE-ACCELERATOR
TRIODE GUN ONLY
2.85 GHz
1.3 GHz
LAWSON-PENNER
ANL (1983)
SLAC INJECTOR (1983)
BOEING-MSNW (1981)
SLAC INJECTOR (1976)
BOEING-MSNW (1983)
LOS ALAMOS NATIONAL LABORATORY (1981)
LOS ALAMOS NATIONAL LABORATORY (1983)
DISPENSER CATHODE
J = 2 A/cm², τ = 3ns
GaAs PHOTO CATHODE
J = 200 A/cm², τ = 30 ps
THERMAL LIMIT
6.2 × 10⁻⁸ Q/√τ
NORMALIZED EMITTANCE, (εx εy / π²)N (cm²·RADIAN²)
Q, CHARGE PER BUNCH (nC)

Fig. 4

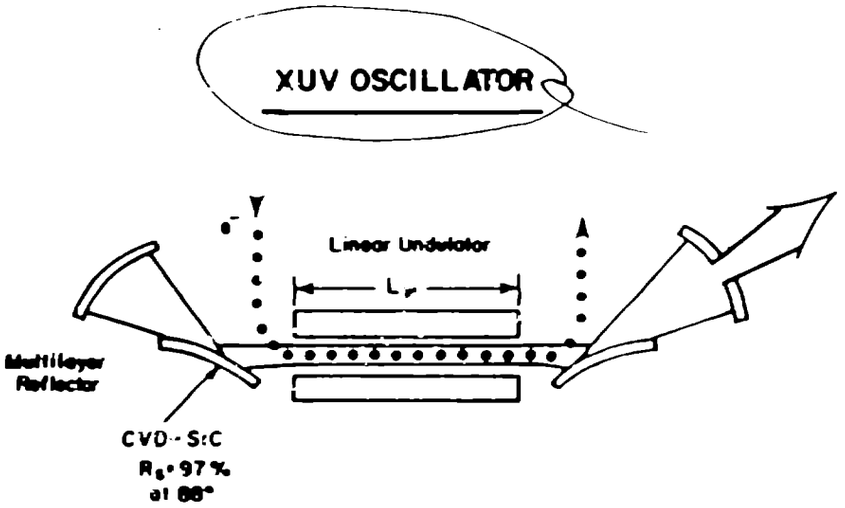
XUV OSCILLATOR
e⁻
Linear Undulator
L_u
Multilayer Reflector
CVD - SiC
R_s = 97 %
at 88°

Fig. 5.

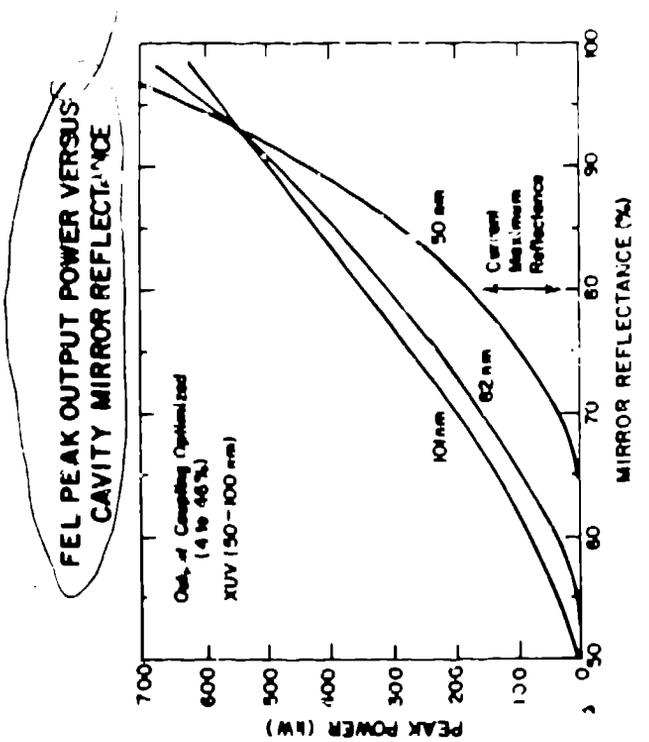
FEL PEAK OUTPUT POWER VERSUS CAVITY MIRROR REFLECTANCE
Output Coupling Optimized (4 to 46%)
XUV (50–100 nm)
50 nm
82 nm
101 nm
Current Maximum Reflectance
PEAK POWER (MW)
MIRROR REFLECTANCE (%)
700
600
500
400
300
200
100
0
50
60
70
80
90
100

Fig. 6.